



Sum Rate Optimization Scheme of UAV-Assisted NOMA under Hardware Impairments

Xiaoyu Wan ^{1,2}, Xiongqing Yang ¹, Zhengqiang Wang ^{1,*}, Zifu Fan ¹ and Bin Duo ³

¹ School of Communication and Information Engineering, Chongqing University of Posts and Telecommunications, Chongqing 400065, China

² Key Laboratory of Electronic Commerce and Modern Logistics, Chongqing Education Commission, Chongqing 400065, China

³ College of Computer Science and Cyber Security, Chengdu University of Technology, Chengdu 200433, China

* Correspondence: wangzq@cqupt.edu.cn; Tel.: +86-151-2300-9069

Abstract: In the unmanned aerial vehicle (UAV) assisted non-orthogonal multiple access (NOMA) networks, the practical hardware impairments (HIs) and resource allocation is still a challenging problem. Most existing research on resource allocation algorithms for UAV communication is considered with the ideal hardware condition. However, the impact of HIs on system performance cannot be ignored, especially in the case of high bit rates. Considering the HIs, most studies are from the perspective of performance analysis. The resource allocation of UAV relay-assisted NOMA systems is investigated in this paper with HIs. We aim to maximize the sum rate by jointly optimizing the deployment of UAV and transmit power. To address this problem, we first transformed the mixed integer programming problem (MIPP) into a standard convex optimization problem based on successive convex approximation (SCA) technology. Then, we introduced the Lagrangian dual transformation and quadratic transform methods to solve the power allocation problem. Finally, we propose an effective iterative algorithm to achieve an approximate optimal solution. Numerical results demonstrate that the proposed algorithm achieved better performance in terms of the sum rate compared with other benchmark schemes.



Citation: Wan, X.; Yang, X.; Wang, Z.; Fan, Z.; Duo, B. Sum Rate Optimization Scheme of UAV-Assisted NOMA under Hardware Impairments. *Appl. Sci.* **2023**, *13*, 2971. <https://doi.org/10.3390/app13052971>

Academic Editors: Paulo M. Mendes, Jose Cabral and Hugo Daniel da Costa Dinis

Received: 25 December 2022

Revised: 18 February 2023

Accepted: 23 February 2023

Published: 25 February 2023



Copyright: © 2023 by the authors. Licensee MDPI, Basel, Switzerland. This article is an open access article distributed under the terms and conditions of the Creative Commons Attribution (CC BY) license (<https://creativecommons.org/licenses/by/4.0/>).

Keywords: UAV; NOMA; resource allocation; hardware impairments; quadratic transform

1. Introduction

1.1. Background

Future sixth-generation (6G) communication requires a higher performance index, such as hyper-scale connectivity and ultra-high message transmission rates [1]. To meet the performance requirements, non-orthogonal multiple access (NOMA) as a promising candidate technology has aroused wide attention due to its characteristics for improving spectrum efficiency and system capacity [2,3]. The dominant advantage of NOMA is to allow the multi-user sharing of the same time, frequency, and code domain resources by overlapping power domains at transmitters. At the receivers, and according to the receipt, power signals can decode the superimposed information with successive interference cancellation (SIC) technology [4].

Meanwhile, unmanned aerial vehicle (UAV) communication is a new developing technology that can help NOMA obtain a preferable performance because of its high maneuverability and low overhead. UAVs provide a wider coverage range and larger throughput as flying relays for wireless communications [5,6]. The authors in [7] studied the optimum altitude of UAV by considering the total power loss, outage probability, and bit error rate. Ref. [8] proposed an iterative method to obtain the locally optimal throughput and analyzed the algorithm's complexity by considering a moving relay system assisted by a UAV with a finite buffer. The authors first derived the closed-form expression of

transmitted power and then proposed a fractional programming-based suboptimal algorithm in [9]. The authors in [10] used a weighted K-means approach for drone deployment and proposed a Q-learning algorithm to optimize content placement. Ref. [11] focused on a multi-UAV-assisted wireless network, solving cache placement, trajectory, and power allocation problems in an iterative method to maximize the minimum throughput for UAV service users. The authors optimized the location of the optimal UAV base station under the coverage probability constraint by using the Gray Wolf optimization algorithm in [12].

1.2. Related Works and Motivation

The joint NOMA and UAV technology was investigated in [13–20] to improve the system's performance further. The study in [13] provided a closed-form expression of outage probability and ergodic capacities in UAV-aided relay NOMA networks. In [14], the sum rate of downlink users was maximized by jointly optimizing the position and power of the UAV. Ref. [15] investigated a multi-user NOMA system with a flying base station (BS). The authors obtained globally optimal solutions to both problems for the placement of UAV and its power allocation. In [16], the authors proposed a path-following method to solve the max-min rate optimization problem in UAV-enabled BS networks. In [17], BS and UAV cooperated to serve ground users simultaneously and employed the method of an iterative algorithm to complete the sum rate maximization problem. Ref. [18] showed an iterative method that could achieve an approximate optimal solution of joint optimization maximization throughput problem in multiple user group NOMA networks with a UAV relay. In [19], a block coordinate descent method was used to solve a minimum energy consumption problem in the uplink NOMA communication for a UAV-assisted base station system. The authors proposed a method combining NOMA and spatial modulation to improve the energy efficiency of UAV in [20]. The aforementioned work in [13–20] presumed that the hardware condition in the system was ideal.

In practical UAV-aided NOMA systems, The communication node takes the form of suffering hardware impairments (HIs), which consist of an in-phase/quadrature-phase imbalance (IQI), radio frequency circuit noise, and non-linear amplifiers equivalent noise [21,22]. The performance analysis was conducted for the UAV communication network under HIs in [23–25]. In [23], the average sum rate was asymptotically analyzed for UAV-assisted NOMA multi-way relaying networks with hardware impairments in the Nakagami-m fading channel. In [24], the outage probability was derived for the satellite-unmanned aerial vehicle (UAV)-terrestrial networks with a reconfigurable intelligent surface under hardware impairments. In [25], the asymptotic outage behavior was investigated for a hybrid satellite-terrestrial network aided by UAV relays under hardware impairments.

Although NOMA and UAV have been studied in previous works [23–25] for performance analysis, very little attention has been paid to the resource allocation problems of the UAV-assisted NOMA communication network. In [26]'s study on the fair allocation of resources for cooperative and cognitive NOMA networks with hardware impairment, the authors derived the closed-form optimal power and time slots allocation. The difference between this paper and [26] is that the UAV relay adopts the decode-and-forward protocol, and the system max-min fair fitness is studied under the assumption that the user channel gain is sorted in advance in [26]. However, in this paper, under the condition of hardware impairments, the UAV adopts the amplify-and-forward protocol and considers the variable order of the user channel gain to study the system sum rate. Our research considers more complex network scenarios and is more in line with the actual situation. A comparison of the related UAV's works is summarized in Table 1.

Table 1. Comparison of the related UAV's works.

Objective	HIs	Model	UAV Relay	Article
Sum Rate	×	LoS	×	[9]
Performance Analysis	×	Rician	✓	[13]
Sum Rate	×	LoS	×	[14]
Achievable Rate	×	LoS	×	[15]

Table 1. Cont.

Objective	HIs	Model	UAV Relay	Article
Max-min Rate	×	Rician	×	[16]
Sum Rate	×	LoS	×	[17]
Total Transmit Energy	×	LoS	✓	[19]
Energy Efficiency	×	LoS&NLoS	×	[20]
Performance Analysis	✓	Nakagami-m	✓	[23]
Performance Analysis	✓	Nakagami-m	✓	[25]
Max-min Rate	✓	LoS&NLoS	✓	[26]
Average Request Delay	×	LoS&NLoS	×	[10]
Max-min Rate	×	LoS	✓	[11]
Coverage probability	×	LoS&NLoS	×	[12]
Sum rate	✓	LoS	✓	This Work

1.3. Contributions and Organization

Motivated by previous work, the UAV's deployment location and resource allocation were considered in a NOMA communication network with imperfect hardware conditions. Particularly, we focused on a system's sum rate optimization problem subject to multiple ground users' minimum rate threshold and power constraints. Furthermore, UAVs can present flexible deployment and the SIC decoding order changes with the position of the drone. A binary decoding decision variable, which represents channel coefficient relationships between the UAV and ground multi-users, was introduced to this problem. On the other hand, the proposed optimization problem was a mixed integer programming problem that was hard to handle directly. Therefore, we proposed an effective iterative algorithm based on variable substitution, successive convex approximation (SCA) method, and quadratic transform algorithm to handle this problem. Numbers of the simulation results show that the proposed scheme can always achieve the optimal system's sum rate performance in the presence of hardware impairments when compared with other comparison schemes. Finally, the feasibility and effectiveness of the proposed algorithm were proved.

2. System Model and Problem Formulation

The NOMA-based UAV communication model with HIs is shown in Figure 1. We consider a UAV half-duplex relaying NOMA networks consisting of a BS and a rotor-wing UAV work in the amplify-and-forward (AF) mode, which assists data transmission from BS to downlink users. All communication nodes are equipped with a single antenna.

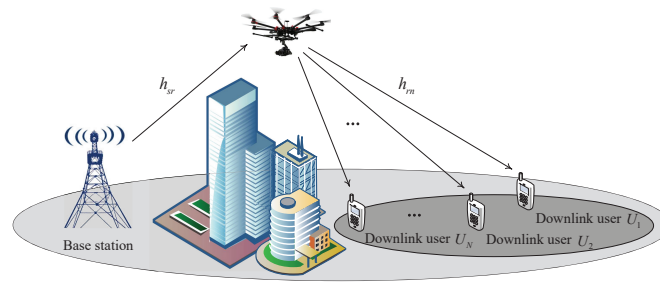


Figure 1. NOMA-based UAV communication model with HIs.

The ground users $U_n, n \in \{1, 2, \dots, N\}$ are located at $I_n = [w_n^T, 0]^T$, where the horizontal coordinates are represented by $w_n = [x_n, y_n]^T$. The coordination of BS is $I_{BS} = [w_s^T, 0]^T$; similarly, $w_s = [x_s, y_s]^T$. The UAV flies on the horizontal plane at a fixed height H . $I_r = [w_r^T, H]^T$ denotes the horizontal coordinate of UAV, where $w_r = [x, y]^T$. According to the 3GPP report, the LoS probability is nearly 100% when the drone is above 100m height from the ground in the urban macro scenario [27,28]. Thus, a free-space path loss model is considered between the UAV and ground users due to channels being dominated by line-of-sight (LoS) links. Note that this model has been adopted in recent literature such as [29,30]. Hence, the channel gain can be modeled as:

$$h_{sr} = \sqrt{\beta_0 d_{sr}^{-2}} = \sqrt{\frac{\beta_0}{H^2 + (x - x_s)^2 + (y - y_s)^2}}, \tag{1}$$

$$h_{rn} = \sqrt{\beta_0 d_{rn}^{-2}} = \sqrt{\frac{\beta_0}{H^2 + (x - x_n)^2 + (y - y_n)^2}}, \tag{2}$$

where h_{sr} and h_{rn} are the channel coefficients between BS to UAV and UAV to the user n respectively; β_0 denotes the channel gain at the reference distance, d_{sr} and d_{rn} is the distance from BS to UAV and UAV to the user n respectively.

The direct link between the base station and ground users is not considered to be due to a severe shadow effect or building block. The communication process is divided into a two-time slots. In the first slot, the BS sends a superimposed signal $y = \sum_{n=1}^N \sqrt{p_n} \theta_n$ to UAV. The received signal in the UAV can be expressed as:

$$y_r = h_{sr} \left(\sum_{n=1}^N \sqrt{p_n} \theta_n + \eta_{sr} \right) + n_r, \tag{3}$$

where p_n represents the transmitted power of the user n , θ_n is the information symbol of the user n , $n_r \sim \mathcal{CN}(0, \sigma_R^2)$ is the additive white Gaussian noise (AWGN) at UAV, the HIs at both BS and UAV are characterized as independent distortion noise $\eta_{sr} \sim \mathcal{CN}(0, \kappa_{sr}^2 P_s)$, where P_s represents the total power transmitted by BS, $\kappa_{sr}^2 \triangleq \sqrt{\kappa_s^2 + \kappa_r^2}$ represents the total distortion level from BS to the UAV relay, κ_s and κ_r characterize the distortion noise at BS and UAV respectively.

In the second slot, UAV amplifies and forwards the received signal y_r to ground users with amplification gain G as:

$$G = \sqrt{\frac{P_r}{P_s (1 + \kappa_{sr}^2) h_{sr}^2 + \sigma_R^2}}, \tag{4}$$

where P_r denotes the UAV transmitted power.

The received signal at user n can be expressed as:

$$y_{U_n} = h_{sr}h_{rn}G \left(\sum_{i=1}^{n-1} \sqrt{p_i}\theta_i + \sqrt{p_n}\theta_n + \sum_{j=n+1}^N \sqrt{p_j}\theta_j \right) + h_{sr}h_{rn}G\eta_{sr} + h_{rn}Gn_r + h_{rn}\eta_{rn} + n_{U_n}, \tag{5}$$

where $n_{U_n} \sim \mathcal{CN}(0, \sigma_{U_n}^2)$ is the AWGN at the user n , the HIs at both the UAV and user n is characterized as independent distortion noise $\eta_{rn} \sim \mathcal{CN}(0, \kappa_{rn}^2 P_r)$, where $\kappa_{rn}^2 \triangleq \sqrt{\kappa_r^2 + \kappa_n^2}$ represents the total distortion level from UAV to the user n in which κ_r and κ_n characterize the distortion noise at the UAV and user n respectively.

According to the NOMA protocol, the signal receiver of weak users adopts SIC technology. Firstly, the weak users perform successive interference cancellations from the received signal, and the strong user’s signal is regarded as interference to the weak users. Therefore, we introduced the binary variable $\alpha_{k,n} \in \{0, 1\}, \forall k, n$ to denote the SIC decoding order. When $\alpha_{k,n} = 1$, the user k with a stronger channel gain is treated as interference to decode the user n . $\alpha_{k,n} = 0$ to present other situations. Thereby, $\alpha_{k,n}$ is defined as:

$$\alpha_{k,n} = \begin{cases} 1, d_k < d_n \\ 0, d_k > d_n \\ 0 \text{ or } 1, d_k = d_n \end{cases}, \forall k, n. \tag{6}$$

Nevertheless, $\alpha_{k,n}$ is an integral binary variable. For ease of explosion, we can rewrite (6) as follows:

$$\alpha_{k,n} \in \{0, 1\}, \forall k \neq n, \tag{7a}$$

$$\alpha_{n,n} = 0, \forall n, \tag{7b}$$

$$\alpha_{k,n} + \alpha_{n,k} = 1, \forall k \neq n, \tag{7c}$$

$$\alpha_{k,n}d_{rk}^2 \leq d_{rn}^2, \forall k \neq n. \tag{7d}$$

Note that (7b) means that the user n decoding its signal should not regard itself as interference. (7c) means that two different users must be able to be divided into a strong user and a poor user. (7a), (7c), and (7d) indicate that when $\alpha_{k,n} = 1$, the distance from the user n to the drone is greater than the distance from the user k . Finally, the rate of the user n is defined as:

$$R_n = \frac{1}{2} \log_2 \left(1 + \frac{p_n A_n'}{A_n' \sum_{k \neq n}^N \alpha_{k,n} p_k + A_n B_n + C_n} \right), \tag{8}$$

where

$$A_n = P_s P_r h_{sr}^2 h_{rn}^2,$$

$$A_n' = P_r h_{sr}^2 h_{rn}^2,$$

$$B_n = \kappa_{sr}^2 + \kappa_{rn}^2 + \kappa_{rn}^2 \kappa_{sr}^2,$$

$$C_n = P_s h_{sr}^2 (1 + \kappa_{sr}^2) \sigma_{U_n}^2 + P_r h_{rn}^2 (1 + \kappa_{rn}^2) \sigma_R^2 + \sigma_R^2 \sigma_{U_n}^2.$$

Problem Formulation

As stated above, the system’s sum rate optimization problem can be modeled as:

P1 :

$$\begin{aligned} & \max_{P_s, P_r, x, y, \mathbf{A}, \mathbf{P}} \sum_{n=1}^N \frac{1}{2} \log_2 \left(1 + \frac{p_n A_n'}{A_n' \sum_{k \neq n}^N \alpha_{k,n} p_k + A_n B_n + C_n} \right) \\ & \text{s.t. } 0 \leq p_n, \forall n, \tag{9a} \\ & \sum_{n=1}^N p_n \leq P_s, \tag{9b} \\ & 0 \leq P_r \leq P_r^{\max}, \tag{9c} \\ & 0 \leq P_s \leq P_s^{\max}, \tag{9d} \\ & p_n - \sum_{k \neq n}^N \alpha_{k,n} p_k \geq 0, \forall n, \tag{9e} \\ & R_n^{\min} \leq R_n, \forall n, \tag{9f} \\ & (7a)-(7d). \end{aligned}$$

where (9a) indicates the non-negative power constraint, (9b) indicates the constraint of the total transmitted power, (9c) and (9d) represent the maximum transmitted power constraint for UAV and BS, respectively, (9e) indicates the user fairness as [31], and (9f) shows the minimum rate constraint for each user.

Since the objective optimization problem P1 increases monotonically with respect to P_s and P_r , we can solve the sum rate maximization problem at P_s^{\max} and P_r^{\max} .

3. Optimization of UAV Position and Power Allocation

In this section, an iterative algorithm is proposed to solve P1. Firstly, we optimized the position of the UAV by transforming the non-convex optimization problem with a fixed power allocation into a convex problem by employing SCA and variable substitution. Secondly, we obtained the power allocation with a quadratic transform method effectively. Finally, we continuously updated the variable block \mathbf{A} , (x, y) and \mathbf{P} alternatively to obtain the solution of P1.

3.1. Uav Position Optimization

For the non-convex constraint (7a) which is equivalent to:

$$0 \leq \alpha_{k,n} \leq 1, \forall k, n, \tag{10a}$$

$$\alpha_{k,n} - \alpha_{k,n}^2 \leq 0, \forall k, n. \tag{10b}$$

the inequality (10a) is affine, but the constraint (10b) is still non-convex, which can be transformed into a convex one through the use of SCA. Constraint (10b) can be rewritten as:

$$\alpha_{k,n} \leq \bar{\alpha}_{k,n}^2 + 2\bar{\alpha}_{k,n}(\alpha_{k,n} - \bar{\alpha}_{k,n}), \forall k, n. \tag{11}$$

The objective function in P1 with a fixed power allocation is still hard to handle because it does not have a strictly concave-convex form that can be directly handled by

fractional programming. Thus we introduced non-negatively auxiliary variables $\mathbf{R}, \mathbf{T}, \forall n$. It can be rewritten as:

$$P2 : \tag{12a}$$

$$\begin{aligned} & \max_{x,y,A,T,R} \sum_{n=1}^N R_n \\ & \text{s.t. } \frac{1}{2} \log_2 \left(1 + \frac{p_n}{t_n} \right) \geq R_n, \forall n, \end{aligned} \tag{12b}$$

$$t_n \geq \sum_{k \neq n}^N \alpha_{k,n} p_k + \frac{A_n B_n + C_n}{A_n'}, \forall n, \tag{12c}$$

$$(7b)-(7d), (9f), (10a), (11).$$

P2 is hard to solve due to the non-convex constraints (9f), (12b), and (12c). By performing mathematical operations to (12b) and applying a first-order Taylor expansion, (12b) can be given as follows:

$$\log_2(t_n + p_n) - \log_2(\bar{t}_n) - \frac{\log_2 e}{\bar{t}_n} (t_n - \bar{t}_n) \geq 2R_n, \forall n. \tag{13}$$

With some simple mathematical transformations and the SCA technique at the first term on the right side of (12c), we obtained:

$$\sum_{k \neq n}^N \alpha_{k,n} p_k \leq \frac{1}{4} \sum_{k \neq n}^N \Pi_{k,n}, \tag{14}$$

where

$$\Pi_{k,n} = (\alpha_{k,n} + p_k)^2 - (\bar{\alpha}_{k,n} - p_k)^2 - 2(\bar{\alpha}_{k,n} - p_k)(\alpha_{k,n} - \bar{\alpha}_{k,n}).$$

By substituting A_n, A_n', B_n, C_n into the second term on the right side of (12c), it could be formulated through the following:

$$\frac{A_n B_n + C_n}{A_n'} = \frac{P_s (1 + \kappa_{sr}^2) \sigma_{U_n}^2}{P_r \beta_0} d_{rn}^2 + \frac{(1 + \kappa_{rn}^2) \sigma_R^2}{\beta_0} d_{sr}^2 + \Lambda (\mathcal{V} - D_{rn} D_{sr}) + P_s B_n, \tag{15}$$

where

$$\begin{aligned} \mathcal{V} &= H^4 + H^2 D_{rn} + H^2 D_{sr}, \\ \Lambda &= \frac{\sigma_R^2 \sigma_{U_n}^2}{P_r \beta_0^2}, \\ d_{rn}^2 &= H^2 + D_{rn}, \\ d_{sr}^2 &= H^2 + D_{sr}, \\ D_{sr} &= (x - x_s)^2 + (y - y_s)^2, \\ D_{rn} &= (x - x_n)^2 + (y - y_n)^2. \end{aligned}$$

Since the second term appeared to be the convex multiplied by the convex, we employed the scaling method to solve this problem. The non-convex term $D_{rn} D_{sr}$ can be scaled as:

$$D_{rn} D_{sr} \leq e^{f_n(x,y)}, \tag{16}$$

where

$$f_n(x, y) = (x - \bar{x}) \frac{2(\bar{x} - x_s)}{\Psi} + (y - \bar{y}) \frac{2(\bar{y} - y_s)}{\Psi} + (x - \bar{x}) \frac{2(\bar{x} - x_n)}{\Theta_n} + (y - \bar{y}) \frac{2(\bar{y} - y_n)}{\Theta_n} + \ln(\Psi) + \ln(\Theta_n),$$

$$\Psi = (\bar{x} - x_s)^2 + (\bar{y} - y_s)^2, \Theta_n = (\bar{x} - x_n)^2 + (\bar{y} - y_n)^2.$$

From the above discussion, constraint (12c) can be rewritten as:

$$t_n \geq \Phi(x, y, \mathbf{A}), \forall n, \tag{17}$$

where

$$\Phi(x, y, \mathbf{A}) = \frac{1}{4} \sum_{k \neq n}^N \Pi_{k,n} + P_s B_n + \Lambda \left(\mathcal{V} + e^{f_n(x,y)} \right) + \frac{P_s (1 + \kappa_{sr}^2) \sigma_{U_n}^2}{P_r \beta_0} d_{rn}^2 + \frac{(1 + \kappa_{rn}^2) \sigma_R^2}{\beta_0} d_{sr}^2.$$

Similarly, constraint (9f) can be rewritten as:

$$\left(2^{R_n^{\min}} - 1 \right) \Phi(x, y, \mathbf{A}) \leq p_n, \forall n. \tag{18}$$

Problem P2 can then be rewritten as:

P3 :

$$\max_{x,y,\mathbf{A},\mathbf{T},\mathbf{R}} \sum_{n=1}^N R_n \tag{19}$$

s.t. (7b)–(7d), (10a), (11), (13), (17), (18).

P3 can be handled by the interior-point method or the standard convex optimization solver, including the CVX toolbox.

3.2. Power Allocation Optimization

The sum rate maximization problem can be rewritten as follows when the UAV’s position is fixed.

P4 :

$$\max_{\mathbf{P}} \frac{1}{2} \sum_{n=1}^N \log_2 \left(1 + \frac{p_n A_n'}{A_n' \sum_{k \neq n}^N \alpha_{k,n} p_k + A_n B_n + C_n} \right) \tag{20}$$

s.t. (9a)–(9b), (9e)–(9f).

P4 is hard to handle due to its objective function and is not strictly concave-convex according to the Lagrangian dual transform technique proposed in [24]. The optimization problem in P4 can be expressed as:

$$\max_{\mathbf{Y}, \mathbf{P}} \frac{1}{2} g(\mathbf{P}, \mathbf{Y}). \tag{21}$$

where \mathbf{Y} refers to (Y_1, \dots, Y_N) and Y_n is introduced as the auxiliary variable and was introduced for each ratio term in the objective function in P4, and

$$g(\mathbf{P}, \mathbf{Y}) = \sum_{n=1}^N \log_2(1 + Y_n) - \sum_{n=1}^N Y_n + \sum_{n=1}^N \frac{(1 + Y_n)p_n A_n'}{\underbrace{p_n A_n' + A_n' \sum_{k \neq n}^N \alpha_{k,n} p_k + A_n B_n + C_n}_{\text{sum-of-ratioterm}}}. \tag{22}$$

By setting $\partial g / \partial Y_n = 0$, we can obtain:

$$Y_n^* = \frac{\log_2 e (p_n A_n') + b \left(A_n' \sum_{k \neq n}^N \alpha_{k,n} p_k + A_n B_n + C_n \right)}{A_n' \sum_{k \neq n}^N \alpha_{k,n} p_k + A_n B_n + C_n}. \tag{23}$$

where $b = \log_2 e - 1$.

By substituting (23) into (22) and adopting a quadratic transform algorithm in [32], the sum-of-ratio term can be solved in (22). Finally, the objective function in P4 can be transformed into:

$$g(\mathbf{P}, \mathbf{Y}^*, \mathbf{Z}) = \sum_{n=1}^N \log_2(1 + Y_n^*) - \sum_{n=1}^N Y_n^* + \sum_{n=1}^N \left(2Z_n \sqrt{(1 + Y_n^*)p_n A_n'} - Z_n^2 \Xi(\mathbf{P}) \right), \tag{24}$$

where $\Xi(\mathbf{P}) = p_n A_n' + A_n' \sum_{k \neq n}^N \alpha_{k,n} p_k + A_n B_n + C_n$.

We can obtain the following closed-form solution for variable \mathbf{Z}

$$Z_n^* = \frac{\sqrt{(1 + Y_n^*)p_n A_n'}}{\left(p_n A_n' + A_n' \sum_{k \neq n}^N \alpha_{k,n} p_k + A_n B_n + C_n \right)}. \tag{25}$$

Finally, by substituting (25) into (24), P3 can be rewritten as the standard convex optimization problem.

$$\begin{aligned} \text{P5 : } \max_{\mathbf{P}} \quad & \frac{1}{2} g(\mathbf{P}, \mathbf{Y}^*, \mathbf{Z}^*) \\ \text{s.t. } \quad & (9a)-(9b), (9e)-(9f). \end{aligned} \tag{26}$$

It can be handled by the interior-point method. In the following, we propose an algorithm with which to solve the sum rate optimization problem effectively.

4. Proposed Algorithm and Complexity Analysis

We analyzed the complexity of our proposed algorithm. We assumed that the number of iterations was K and the number of users in the communication system was N . In each iteration, the sum rate optimization problem was handled by solving P3 and P5 alternatively. Due to the fact that they are coupled, the complexity of P3 was $O\left(\left((x^2 y + x^3) y^{1/2}\right) \log\left(\frac{1}{\varepsilon}\right)\right)$, where $x = N^2 + 2N + 2$ variables and $y = \frac{7}{2}N^2 + \frac{5}{2}N$ constraints. ε is the tolerance error value in the interior-point method [33]. Thereby, the complexity of our proposed algorithm was $O\left(KN^7 \log\left(\frac{1}{\varepsilon}\right)\right)$. The details of Algorithm 1 are shown as follows:

Algorithm 1 Iterative Algorithm for P1

- 1: Initialize $\mathbf{P}^0, (x^0, y^0), (x_s, y_s), (x_n, y_n)$ and generate \mathbf{A}^0 .
 - 2: Let iterative index $l = 0$ and tolerance $\delta > 0$.
 - 3: Repeat
 - STEP1: Solve convex problem P3 through the interior-point method by giving \mathbf{P}^l and obtaining the solution $\mathbf{A}^{l+1}, (x^{l+1}, y^{l+1})$.
 - STEP2: Update \mathbf{Y}_n^{l+1} and \mathbf{Z}_n^{l+1} by (23) and (25) respectively.
 - STEP3: Update \mathbf{P}^{l+1} by solving convex problem P5.
 - STEP4: Update the iterative index $l = l + 1$.
 - 4: Until $R_{sum}^{l+1} - R_{sum}^l < \delta$.
 - 5: Output: $\mathbf{P}, \mathbf{A}, (x, y)$.
-

5. Simulation Results

In this part, we measure the system performance of our proposed placement and power allocation iterative algorithm by numerical results. We consider a NOMA-based downlink UAV relaying networks scene where the coordinate of BS is set as $I_{BS} = [0, 0]^T$, and the users are randomly distributed over a 300 m × 300 m geometric region with the geometric center [150 m, 150 m]. We set the power of AWGN $\sigma_R^2 = \sigma_{U_n}^2 = 10^{-11}$ W, $R_n^{\min} = 0.5$ bps/Hz, $\beta_0 = 10^{-3}$, and assumed that UAV and users both suffered the same grade HIs. Figure 2 illustrates the different UAV deployment locations when the system $P_s = 2$ W, $P_{UAV} = 0.03$ W, $H = 100$ m and 8 downlink users exist in the system. The key parameter settings are summarized in Table 2.

Figure 3 shows the convergence performance of iterations with a fixed UAV height 100 m and $P_{UAV} = 0.03$ W, BS with maximum power $P_s = 2$ W and 3 randomly deployed users. It can be concluded from the simulation figure that the proposed algorithm could converge to the optimal value within three times in the worst case, which verifies the effectiveness and rapid convergence of the proposed iterative algorithm. When the HIs increase at equal intervals, the system performance worsens.

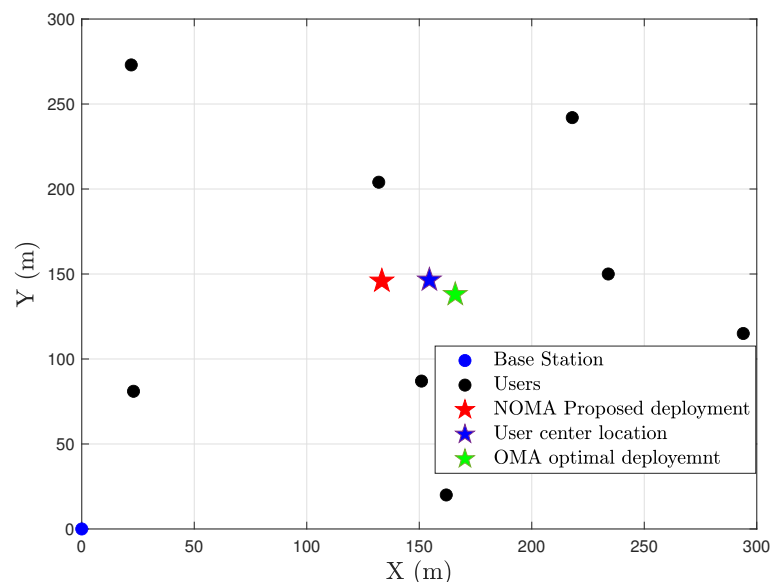


Figure 2. System user’s distribution versus the different scheme of UAV deployment.

Table 2. Simulation parameters.

Base station transmit maximum power P_S	2 W
UAV transmit maximum power P_{UAV}	0.1 W
AWGN $\sigma_R^2, \sigma_{U_n}^2$	10^{-11} W
The flight height H	100–120 m
QoS R_n^{\min}	0.5 bps/Hz
Channel power gain β_0 at a distance of 1 m	−30 dB
Coverage area of UAV	300 m × 300 m

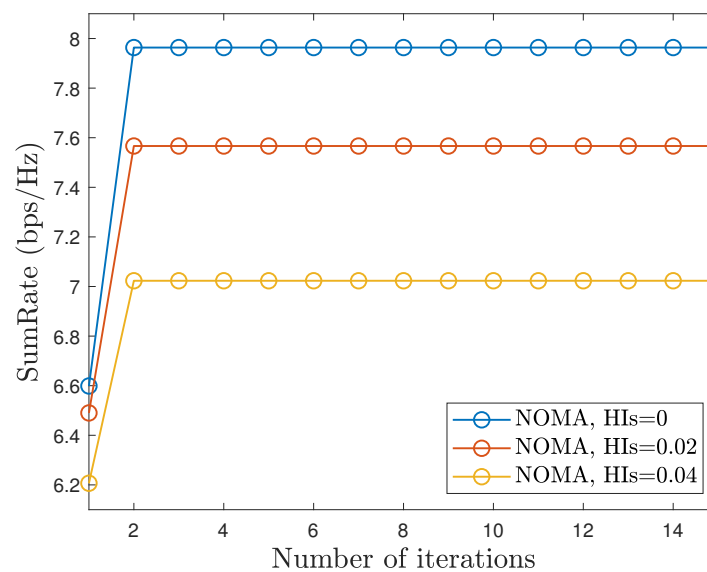


Figure 3. System downlink sum rate versus the number of iterations.

Figure 4 shows the system downlink sum rate versus P_{UAV} with a UAV height of 100 m, BS with maximum power $P_S = 2$ W and three randomly deployed users. We compared the proposed scheme with a scheme that deploys the UAV to optimize the power allocation at the user’s geometric center location and an average power allocation scheme that optimizes the UAV deployment location. As we expected, the sum rate of the different schemes suffering from different degrees of HIs increased with the increment transmitted power of UAV, and The proposed scheme always achieves the maximum sum rate performance with the same degree of hardware impairments. It is noteworthy that the impact of the UAV’s deployment location on the system’s sum rate was more significant than that of the fixed deployment location optimized power scheme with fewer hardware impairments. This impact was diminished as the hardware impairments level increased.

Figure 5 shows the system downlink sum rate versus P_S with a UAV height of 100 m, UAV with maximum power $P_{UAV} = 0.03$ W, and three randomly deployed users. The simulation results indicate that the proposed scheme exhibited a trend of initial rapid increase followed by gradual growth with respect to the base station power. It can also be observed that the extent of the hardware impairments was exacerbated, and the sum rate performance of the system decreased. A lower maximum base station transmission power led to a greater impact on the system’s sum rate when considering the constant maximum transmission power of the UAV. On the other hand, increasing the transmission power of the UAV with a constant maximum base station transmission power resulted in an enhanced system’s sum rate. Nevertheless, it should be noted that an intensification of hardware impairments led to a reduction in differentials.

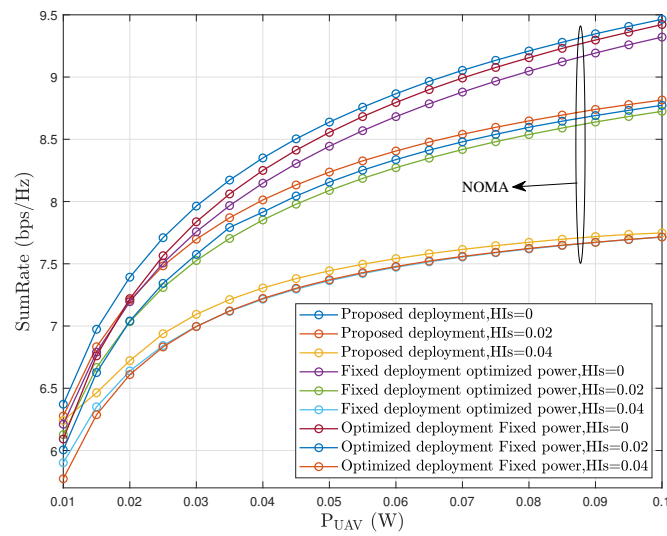


Figure 4. System downlink sum rate versus the maximum power of UAV.

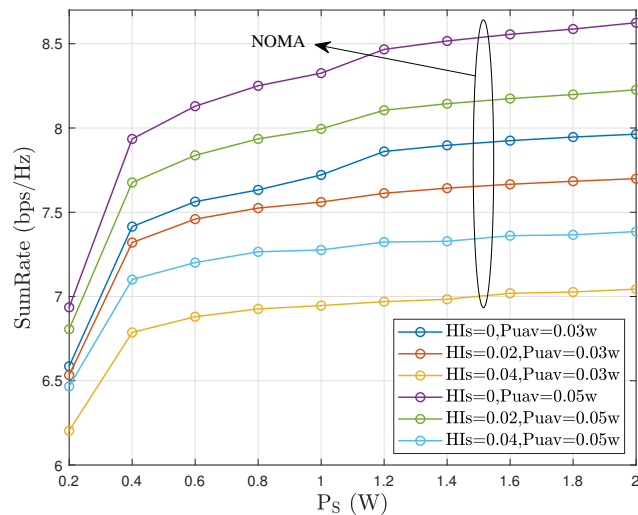


Figure 5. System downlink sum rate versus the maximum power of BS with different HIs.

Figure 6 indicates the system downlink sum rate versus a different number of users with $P_s = 2\text{ W}$, $P_{UAV} = 0.05\text{ W}$; the height of the drone was 100 m. We compared the optimization power allocation NOMA scheme for drone deployment at the user’s geometric center and the OMA scheme for optimal location optimization power allocation. In the scheme where the drone was deployed at the user’s geometric center with optimized power under ideal hardware conditions, the performance obtained by the system was only slightly higher than that obtained by the proposed scheme when $HIs = 0.02$, demonstrating the effectiveness of the proposed algorithm. In the case of NOMA, the sum rate increased when the power allocation meet the QoS requirements of all the admitted users. The sum rate decreased with the number of users increased. This is because the transmitted power was not large enough to satisfy the demand of each user. In the case of OMA, the system’s sum rate deteriorated as the number of users increased. The performance of the power-optimized OMA scheme at the optimal location degraded by about 45% compared to the system’s sum rate that was obtained with the proposed NOMA scheme with ideal hardware.

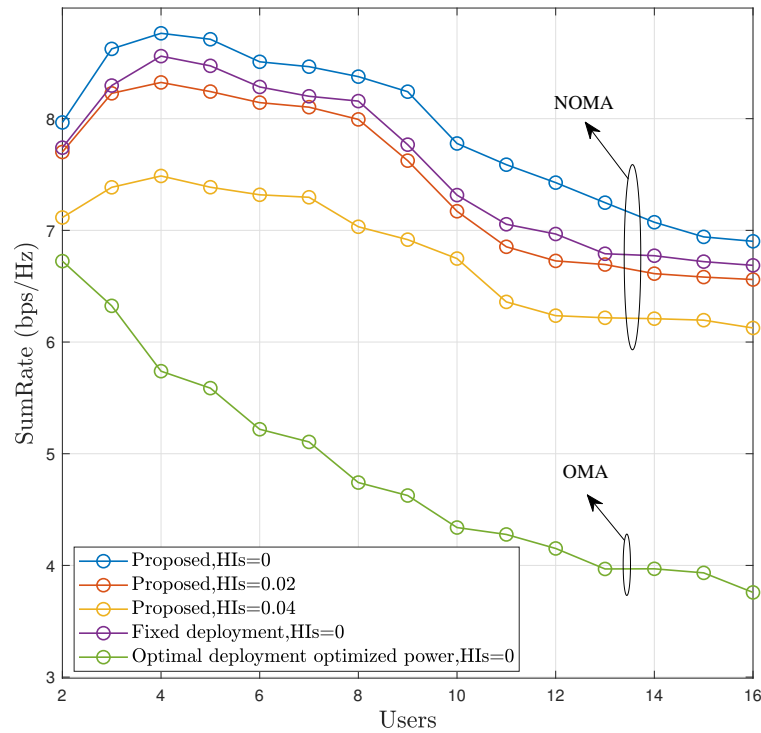


Figure 6. System downlink sum rate versus the number of users.

Figure 7 shows the total system downlink rate versus the deployed UAV at different altitudes for different schemes with $P_s = 2\text{ W}$, $P_{UAV} = 0.03\text{ W}$, three downlink users, and HIs of 0.02. We compared the NOMA scenario, which included the UAV deployed at the geometric center of the user with optimized power and average power, and the OMA scenario, which included the UAV deployed at the optimal location of the UAV using optimized power and average power. It can be seen from the results that the performance of all schemes tended to decrease as the UAV altitude increased, which was because the corresponding channel gain became worse as the distance between the UAV and the ground user increased. Still, the proposed scheme always achieved optimal performance.

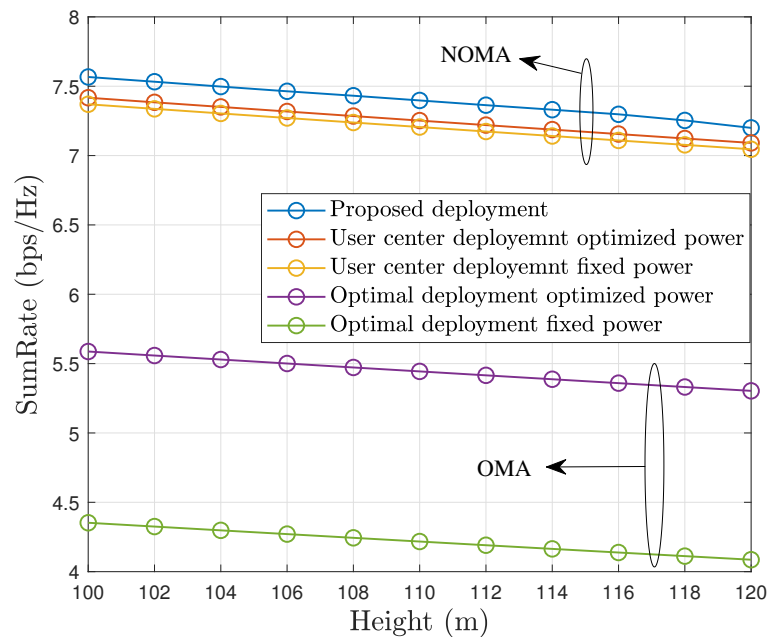


Figure 7. System downlink sum rate versus the altitude of UAV.

Figure 8 shows the system downlink sum rate versus P_S under different schemes, where the UAV height was 100 m, $HIs = 0.02$, UAV with maximum power $P_{UAV} = 0.03$ W, and three randomly deployed users. With the same level of hardware impairments, the system’s sum rate obtained for all schemes increased as the base station transmit power increased. Because base stations transmit more power, the system can allocate more power to each user. In addition, the optimal performance was always obtained for our proposed scheme because it optimized both the UAV deployment location and the user power allocation while considering the hardware impairments.

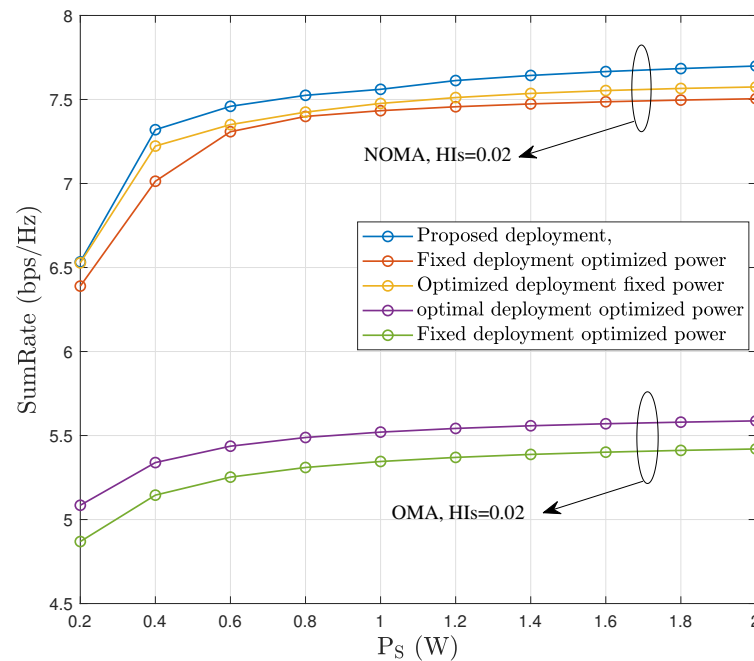


Figure 8. System downlink sum rate versus the maximum power of BS with same HIs.

Figure 9 shows the system downlink sum rate versus P_{UAV} with a UAV height of 100 m, BS with maximum power $P_S = 2$ W, $HIs = 0.02$, and three randomly deployed users. We compared the proposed scheme with the NOMA scheme and optimized average power at the UAV deployment location and the NOMA scheme with an optimized power allocation to deploy the UAV at the user center, and the OMA scheme with optimized power allocation at the optimal deployment location and the OMA scheme with optimized power allocation to deploy the UAV at the user center, respectively. This scheme jointly considered UAV deployment with system power allocation and always obtained the highest sum rate for the same hardware impairments. Unlike Figure 8, increasing the transmitting power of the UAV achieved a higher and more significant system performance with constant base station power.

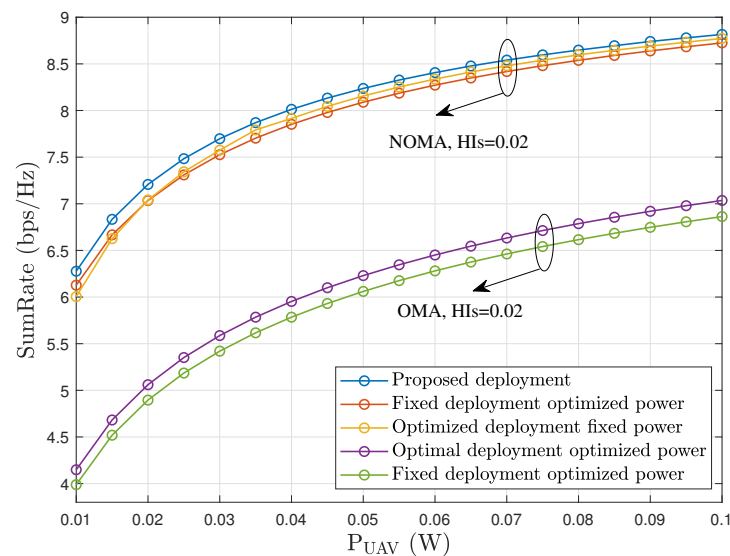


Figure 9. System downlink sum rate versus the maximum power of UAV with the same HIs.

6. Conclusions

This paper has investigated the downlink NOMA networks with an UAV relay. To maximize the sum rate of ground users, we decomposed the optimization problem into UAV location optimization with binary variable constraints and power allocation problems. We first converted the MIPP into a standard convex optimization problem with the SCA method. Then the quadratic transform method and Lagrangian dual transformation were used to obtain the power allocation. Simulation results reveal that our proposed algorithm outperforms other benchmark algorithms. As energy efficiency [34–36] is another crucial index for the future wireless network, we will investigate the energy efficient resource allocation for the UAV-assisted NOMA system in the future. In addition, as the channel between the UAV and users can be with both LoS and NLoS propagation [37,38], we will jointly investigate optimizing the height of the UAV in our future work.

Author Contributions: Conceptualization, methodology, and software, X.W. and Z.W.; validation and investigation, X.Y. and B.D.; writing—original draft preparation, X.Y.; and writing—review and editing, Z.W. and Z.F. All authors have read and agreed to the published version of the manuscript.

Funding: This work was partially supported by the National Natural Science Foundation of China (No. 61701064), Chongqing Natural Science Foundation (No. cstc2019jcyj-msxmX0264), and The Sichuan Regional Innovation Cooperation Project (2022YFQ0017).

Conflicts of Interest: The authors declare no conflict of interest.

References

1. Khan, W.U.; Li, X.; Zeng, M.; Dobre, O.A. Backscatter-enabled noma for future 6G systems: A new optimization framework under imperfect SIC. *IEEE Commun. Lett.* **2021**, *25*, 1669–1672. [[CrossRef](#)]
2. Wang, Z.; Wen, C.; Fan, Z.; Wan, X. A novel price-based power allocation algorithm in Non-Orthogonal Multiple Access Networks. *IEEE Wirel. Commun. Lett.* **2018**, *7*, 230–233. [[CrossRef](#)]
3. Wan, X.-Y.; Chang, R.-F.; Wang, Z.-Q.; Fan, Z.-F. Sum rate maximization for Cooperative Noma with hardware impairments. *IEICE Trans. Inf. Syst.* **2021**, *E104.D*, 1399–1405. [[CrossRef](#)]
4. Islam, S.M.; Avazov, N.; Dobre, O.A.; Kwak, K. Power-domain Non-Orthogonal Multiple Access (NOMA) in 5G systems: Potentials and challenges. *IEEE Commun. Surv. Tutor.* **2017**, *19*, 721–742. [[CrossRef](#)]
5. Amine Ouamri, M.; Alkanhel, R.; Gueguen, C.; Abdullah Alohal, M.; Ghoneim, S.M.S. Modeling and analysis of UAV-assisted mobile network with imperfect beam alignment. *Comput. Mater. Contin.* **2023**, *74*, 453–467. [[CrossRef](#)]
6. Qureshi, H.N.; Imran, A. On the tradeoffs between coverage radius, altitude, and beamwidth for practical UAV deployments. *IEEE Trans. Aerosp. Electron. Syst.* **2019**, *55*, 2805–2821. [[CrossRef](#)]
7. Chen, Y.; Feng, W.; Zheng, G. Optimum placement of UAV as relays. *IEEE Commun. Lett.* **2018**, *22*, 248–251. [[CrossRef](#)]

8. Lee, J.-H.; Park, K.-H.; Ko, Y.-C.; Alouini, M.-S. Throughput maximization of mixed FSO/RF UAV-aided mobile relaying with a buffer. *IEEE Trans. Wirel. Commun.* **2021**, *20*, 683–694. [[CrossRef](#)]
9. Feng, W.; Zhao, N.; Ao, S.; Tang, J.; Zhang, X.; Fu, Y.; So, D.K.; Wong, K.-K. Joint 3D trajectory and power optimization for UAV-aided mmwave MIMO-Noma Networks. *IEEE Trans. Commun.* **2021**, *69*, 2346–2358. [[CrossRef](#)]
10. Luo, J.; Song, J.; Zheng, F.-C.; Gao, L.; Wang, T. User-centric UAV deployment and content placement in cache-enabled Multi-UAV networks. *IEEE Trans. Veh. Technol.* **2022**, *71*, 5656–5660. [[CrossRef](#)]
11. Ji, J.; Zhu, K.; Niyato, D.; Wang, R. Joint Cache Placement, flight trajectory, and transmission power optimization for Multi-UAV Assisted Wireless Networks. *IEEE Trans. Wirel. Commun.* **2020**, *19*, 5389–5403. [[CrossRef](#)]
12. Ouamri, M.A.; Oteşteanu, M.-E.; Barb, G.; Gueguen, C. Coverage Analysis and Efficient Placement of Drone-BSs in 5G Networks. *Eng. Proc.* **2022**, *14*, 18. [[CrossRef](#)]
13. Do, D.-T.; Le, A.-T.; Liu, Y.; Jamalipour, A. User grouping and energy harvesting in UAV-noma system with AF/DF relaying. *IEEE Trans. Veh. Technol.* **2021**, *70*, 11855–11868. [[CrossRef](#)]
14. Liu, X.; Wang, J.; Zhao, N.; Chen, Y.; Zhang, S.; Ding, Z.; Yu, F.R. Placement and power allocation for Noma-UAV Networks. *IEEE Wirel. Commun. Lett.* **2019**, *8*, 965–968. [[CrossRef](#)]
15. Hu, D.; Zhang, Q.; Li, Q.; Qin, J. Joint position, Decoding Order, and power allocation optimization in UAV-based Noma Downlink Communications. *IEEE Syst. J.* **2020**, *14*, 2949–2960. [[CrossRef](#)]
16. Nasir, A.A.; Tuan, H.D.; Duong, T.Q.; Poor, H.V. UAV-enabled communication using noma. *IEEE Trans. Commun.* **2019**, *67*, 5126–5138. [[CrossRef](#)]
17. Zhao, N.; Pang, X.; Li, Z.; Chen, Y.; Li, F.; Ding, Z.; Alouini, M.-S. Joint trajectory and precoding optimization for UAV-assisted Noma Networks. *IEEE Trans. Commun.* **2019**, *67*, 3723–3735. [[CrossRef](#)]
18. Li, B.; Zhang, R.; Yang, L. Joint user grouping and power allocation for noma-based UAV relaying networks. In Proceedings of the 2021 IEEE International Conference on Communications Workshops (ICC Workshops), Montreal, QC, Canada, 14–23 June 2021. [[CrossRef](#)]
19. Xu, W.; Tian, J.; Gu, L.; Tao, S. Joint Placement and Power Optimization of UAV-Relay in NOMA Enabled Maritime IoT System. *Drones* **2022**, *6*, 304. :. 10.3390/drones6100304. [[CrossRef](#)]
20. Jia, M.; Gao, Q.; Guo, Q.; Gu, X. Energy-Efficiency Power Allocation Design for UAV-Assisted Spatial NOMA. *IEEE Internet Things J.* **2021**, *8*, 15205–15215. [[CrossRef](#)]
21. Solanki, S.; Upadhyay, P.K.; da Costa, D.B.; Bithas, P.S.; Kanatas, A.G.; Dias, U.S. Joint IMPACT OF RF hardware impairments and channel estimation errors in spectrum sharing multiple-relay networks. *IEEE Trans. Commun.* **2018**, *66*, 3809–3824. [[CrossRef](#)]
22. Canbilen, A.E.; Ikki, S.S.; Basar, E.; Gultekin, S.S.; Develi, I. Impact of I/Q imbalance on amplify-and-forward relaying: Optimal Detector Design and Error Performance. *IEEE Trans. Commun.* **2019**, *67*, 3154–3166. [[CrossRef](#)]
23. Li, X.; Wang, Q.; Liu, Y.; Tsiftsis, T.A.; Ding, Z.; Nallanathan, A. UAV-aided multi-way NOMA networks with residual hardware impairments. *IEEE Wirel. Commun. Lett.* **2020**, *9*, 1538–1542. [[CrossRef](#)]
24. Guo, K.; An, K. On the performance of RIS-Assisted Integrated Satellite-UAV-terrestrial networks with hardware impairments and interference. *IEEE Wirel. Commun. Lett.* **2022**, *11*, 131–135. [[CrossRef](#)]
25. Sharma, P.K.; Gupta, D. Outage performance of Multi-UAV relaying-based imperfect hardware hybrid satellite-terrestrial networks. *IEEE Syst. J.* **2022**, *16*, 2311–2314. [[CrossRef](#)]
26. Arzykulov, S.; Celik, A.; Naurzybayev, G.; Eltawil, A. UAV-Assisted Cooperative & Cognitive Noma: Deployment, clustering, and resource allocation. *IEEE Trans. Cogn. Commun. Netw.* **2022**, *8*, 263–281. [[CrossRef](#)]
27. Lin, X.; Yajnanarayana, V.; Muruganathan, S.D.; Gao, S.; Asplund, H.; Maattanen, H.-L.; Bergstrom, M.; Euler, S.; Wang, Y.-P.E. The sky is not the limit: LTE for Unmanned Aerial Vehicles. *IEEE Commun. Mag.* **2018**, *56*, 204–210. [[CrossRef](#)]
28. Xu, Y.; Zhang, T.; Yang, D.; Liu, Y.; Tao, M. Joint Resource and trajectory optimization for security in UAV-assisted MEC systems. *IEEE Trans. Commun.* **2021**, *69*, 573–588. [[CrossRef](#)]
29. Xu, Y.; Zhang, T.; Liu, Y.; Yang, D.; Xiao, L.; Tao, M. UAV-assisted MEC networks with aerial and ground cooperation. *IEEE Trans. Wirel. Commun.* **2021**, *20*, 7712–7727. [[CrossRef](#)]
30. Lu, W.; Ding, Y.; Gao, Y.; Chen, Y.; Zhao, N.; Ding, Z.; Nallanathan, A. Secure noma-based UAV-MEC network towards a flying eavesdropper. *IEEE Trans. Commun.* **2022**, *70*, 3364–3376. [[CrossRef](#)]
31. Khan, W.U.; Jameel, F.; Ristaniemi, T.; Khan, S.; Sidhu, G. A.; Liu, J. Joint Spectral and energy efficiency optimization for downlink NOMA Networks. *IEEE Trans. Cogn. Commun. Netw.* **2020**, *6*, 645–656. [[CrossRef](#)]
32. Shen, K.; Yu, W. Fractional Programming for Communication Systems—Part I: Power control and beamforming. *IEEE Trans. Signal Process.* **2018**, *6*, 2616–2630. [[CrossRef](#)]
33. Nesterov, Y.; Nemirovskii, A. *Interior-Point Polynomial Algorithms in Convex Programming*; Society for Industrial and Applied Mathematics: Philadelphia, PA, USA, 1994.
34. Fan, Z.-F.; Cheng, Q.; Wang, Z.-Q.; Meng, X.-H.; Wan, X.-Y. Energy efficient resource allocation for downlink cooperative Non-Orthogonal Multiple Access Systems. *IEICE Trans. Fundam. Electron. Commun. Comput. Sci.* **2018**, *E101.A*, 1603–1607. [[CrossRef](#)]
35. Adam, A. B.; Wan, X.; Wang, Z. Energy efficiency maximization in downlink multi-cell multi-carrier Noma Networks with hardware impairments. *IEEE Access* **2020**, *8*, 210054–210065. [[CrossRef](#)]

36. Wang, Z.; Du, J.; Fan, Z.; Wan, X.; Xu, Y. Energy Efficiency Maximization for multi-carrier cooperative non-orthogonal Multiple Access Systems. *Digit. Signal Process.* **2022**, *130*, 103725. [[CrossRef](#)]
37. Haneya Naeem Qureshi, Marvin Manalastas, Aneeqa Ijaz, Ali Imran, Yongkang Liu, Mohamad Omar Al Kalaa. Communication Requirements in 5G-Enabled Healthcare Applications: Review and Considerations. *Healthcare* **2022**, *10*, 293. [[CrossRef](#)] [[PubMed](#)]
38. Alkama, D.; Ouamri, M.A.; Alzaidi, M.S.; Shaw, R.N.; Azni, M.; Ghoneim, S.S.M. Downlink Performance Analysis in MIMO UAV-Cellular Communication With LOS/NLOS Propagation Under 3D Beamforming. *IEEE Access* **2022**, *10*, 6650–6659. [[CrossRef](#)]

Disclaimer/Publisher's Note: The statements, opinions and data contained in all publications are solely those of the individual author(s) and contributor(s) and not of MDPI and/or the editor(s). MDPI and/or the editor(s) disclaim responsibility for any injury to people or property resulting from any ideas, methods, instructions or products referred to in the content.